Ashdin Publishing
Journal of Drug and Alcohol Research
Vol. 7 (2018), Article ID 236040, 9 pages
doi:10.4303/jdar/236040

Research Article

Alcohol-Induced Hepatic Steatosis: A Comparative Study to Identify Possible Indicator(s) of Alcoholic Fatty Liver Disease

Harshica Fernando,[4] Kamlesh K. Bhopale,[2] Shakuntala S. Kondraganti,[3] Bhupendra S. Kaphalia,[1] and G. A. Shakeel Ansari[1]

[1] *Department of Pathology, The University of Texas Medical Branch, Galveston, TX 77555, USA*
[2] *Department of Internal Medicine, The University of Texas Medical Branch, Galveston, TX 77555, USA*
[3] *Department of Radiology, UT Health Science Center, Houston, TX 77030, USA*
[4] *Department of Chemistry, Prairie View A&M University, 100 University Dr, Prairie View, TX 77446, USA*
Address correspondence to G. A. Shakeel Ansari, sansari@utmb.edu

Received 8 September 2017; Revised 9 December 2017; Accepted 3 January 2018

Abstract *Background.* Fatty liver is an early sign of both nonalcoholic and alcoholic fatty liver diseases. Ethanol feeding using a Lieber-DeCarli liquid diet (LD) model which contains 35% fat to rats or mice is a well-established model for alcoholic fatty liver. However, LD diet alone can also induce fatty liver and its differential metabolic profile may be able to differentiate steatosis induced by LD versus LD plus ethanol. *Purpose.* We investigated the lipidomic differences in the livers of Sprague-Dawley (SD) rats fed a pellet diet (PD), LD, and liquid ethanol diet (LED) for six weeks. *Study design.* Male Sprague Dawley rats were fed with nonalcoholic diets PD, LD or LED (ethanol in LD) for six weeks. Lipids were extracted and analyzed by nuclear magnetic resonance (NMR)-based metabolomics. The NMR data obtained was analyzed by multivariate principal component analysis (PCA) and Spotfire DecisionSite 9.0 software to compare PD versus LD and LD versus LED groups. *Results.* PCA of the NMR spectral data of livers of both comparisons showed a clear separation of PD from LD group and LD from LED group indicating differences in lipid profiles which corresponded with changes in total lipid weights. LD showed increases for cholesterol, esterified cholesterol, cholesterol acetate, and triglycerides with decreases for fatty acyl chain, diallylic, and allylic protons, while the LED showed increases in esterified cholesterol, cholesterol acetate, fatty acid methyl esters, allylic protons, and some triglyceride protons with decreases in free cholesterol and phosphatidylcholine (PC). *Conclusion.* Our data suggest that altered lipid signature or PC levels could be an indicator to differentiate between nonalcoholic versus alcoholic fatty liver.

Keywords alcoholic fatty liver; nonalcoholic fatty liver; steatosis; phosphatidylcholine; lipids

1. Introduction

Hepatic steatosis (fatty liver) is an early sign of nonalcoholic and alcoholic fatty liver diseases (NAFLD and AFLD, resp.), leading to steatohepatitis, fibrosis, and cirrhosis and in some cases hepatocellular carcinoma, if not controlled/reversed. To mimic the alcohol abuse, Lieber-DeCarli liquid diet (LD) has been extensively used in rats/mice. Lieber-DeCarli ethanol liquid diet (LED) model which leads to fatty liver contains $\sim$ 30% fat somewhat similar to the amount consumed by humans [1, 2]. Hence LD itself is capable of inducing steatosis. Therefore, metabolomics is used to distinguish the lipidomic differences by which steatosis is induced by LD and/or LED.

Lipid molecules in living cells, tissues or organisms are critically important for many biological functions. Application of one of the advanced analytical techniques for lipids analyses is "lipidomics". This approach demonstrated a critical role of lipids and lipid-based molecular signatures in many human diseases including diabetes, metabolic syndrome (risk of developing atherosclerosis, inflammation, and hypertension), neurodegenerative disease, and cancer [3]. Lipid dysregulation and its transport appear to be in an early stage of alcoholic liver disease. Lipidomics could identify compositional changes among various lipid classes in nonalcoholic and alcoholic liver diseases which could serve as a diagnostic biomarker for hepatic steatosis and can further support the discovery and development of novel medications for the treatment of alcohol-related adverse conditions.

The metabolome refers to the total metabolites present in a biological sample [4,5]. In order to characterize the metabolites present in a given system (cells, tissues or bio fluids), proton nuclear magnetic resonance spectroscopy (^{1}H-NMR) or mass spectrometry in combination with multivariate statistical analysis has been extensively used [6, 7,8,9,10,11,12]. However, much of the work has been targeted towards identifying the polar metabolites while less attention is given to the lipids, in general, due to the lack of databases for the analysis of specific lipid molecules. Lipids play an important role in energy storage, cellular structure, and signaling. Thus differential distributions of lipids as a result of diet, ethanol or other factors are important in the etiopathogenesis of alcoholic fatty liver. In our previous work, we studied hepatic lipid profiling after ethanol

feeding in rats and mice under various scenarios [13, 14, 15, 16]. The altered lipids were found to be cholesterol, fatty acids, phospholipids, and triglycerides when LD group was compared with LED group. In this study, we investigated the lipidomic differences in the livers of Sprague-Dawley rats fed a pellet diet (PD), LD, and LED for six weeks to evaluate various lipids altered in ethanol-induced fatty liver versus high fat diet using ^{1}H-NMR metabolomics.

2. Materials and methods

2.1. Animals and treatment

Sprague-Dawley (SD) male rats (6–7 weeks old) were purchased from Harlan (Indianapolis, IN, USA). Animal experimentation was performed in accordance with the protocol approved by Institutional Animal Care and Use Committee of the University of Texas Medical Branch, USA, and followed the NIH Guidelines for care and use of laboratory animals. Rats were housed in humidity and temperature-controlled animal room with automatic 12 h light/dark cycles and the experiment was carried out as described previously [13, 14, 15, 16]. After one week of acclimatization, rats were divided into three groups (6–7 animals in each group).

We included PD as a control group fed normal pellet diet, Lieber-DeCarli LD as a high-fat diet group, that can be a surrogate for a NAFLD model, and LD diet with ethanol as an AFLD model. Comparison of these groups provided different lipidomic profiles. We did not include PD + ethanol group in this study because ethanol pair feeding would have included additional variables. The first group was fed with a pellet diet (Prolab RMH 2500, 5P14; Labdiet, St. Louis, MO, USA) (fat 12% calories), and the other animals were pair-fed with a regular Lieber-DeCarli LD (Dyets Cat. #710260, Dyets Inc., Bethlehem, PA, USA) (Carbohydrates (11% of calories), protein (18%), fat (35%)) and alcohol or maltose dextrin (36%) (Dyets Cat. #402851) [17]. The amount of ethanol in the LD was increased gradually from 1% to 5% and then maintained at 5% up to six weeks. The diets were freshly prepared and changed daily with the consumption recorded on daily basis while the weights of animals were recorded on weekly basis. All animals were sacrificed at the end of six weeks by intraperitoneal injection of Nembutal (sodium salt, 100 mg/kg body weight). The blood from each animal was withdrawn from the heart in heparinized tubes, centrifuged at 1,000 g for 10 min to obtain the plasma, and stored at −80 °C until analysis. The livers were harvested and processed as shown in the following subsection.

2.1.1. Liver pathology

The liver from each animal was harvested, grossly examined, and weighed. Two small sections of the liver from the left lobe were cut, one frozen in liquid nitrogen and the other stored in 10% buffered formalin for tissue section cutting and hematoxylin and eosin (H&E) staining and remaining parts of the liver stored at −80 °C. The steatosis was graded by histological examination for accumulation of fat in the hepatocytes and confirmed by Oil Red O staining for lipid deposition as described earlier in [16, 18].

2.1.2. Liver injury markers

The plasma samples were analyzed for hepatic injury markers using alanine aminotransferase (ALT/SGPT Liq-UV), alkaline phosphatase (ALP Liquicolor), and lactic dehydrogenase (LDH-Liq-UV) kits from Stainbio Laboratory, Boerne, TX, USA and aspartate aminotransferase (AST/SGOT) reagent kit from TECO diagnostics, Anaheim, CA, USA as used previously [16].

2.2. Extraction of lipids from livers and NMR analysis

Frozen liver (250 mg) was homogenized in 1.5 mL of methanol and extracted with methyl tert-butyl ether (MTBE) (5 mL) and water (1.25 mL) as described previously [11, 12]. The organic phase was dried under nitrogen to constant weight and the dried residue dissolved in deuterated chloroform containing tetramethylsilane (TMS) as an internal standard (Sigma-Aldrich, WI, USA) [13, 14, 15]. The final volume of the sample was made up to 750 μL in a 5 mm NMR tube (Wilmad Lab glass, NJ, USA). ^{1}H-NMR spectra were obtained using an 800 MHz Varian NMR spectrophotometer (Varian Inc., CA, USA). The chemical shifts of clearly identifiable peaks were assigned to various lipids by comparing the published values on lipids as described previously [13, 14, 15, 19, 20, 21, 22, 23, 24, 25, 26, 27, 28, 29].

2.2.1. Pattern recognition analysis

All ^{1}H-NMR data were reduced to integral regions of equal width of 0.01 ppm using an "in house" VNMR macro and the spectral regions between $\delta = 0.2$ ppm and $\delta = 6.2$ ppm [13, 14]. Baseline corrections were also performed using the same macro. The acquired NMR data were subjected to multivariate statistical analysis. The integrated data were further analyzed using the Spotfire DecisionSite 9.0 software (TIBCO Spotfire, Somerville, MA, USA).

2.3. Statistical analysis

The data were analyzed for statistical significance using Student's t-test and ANOVA or Student-Newman-Keul's multiple comparison tests and P value ≤ 0.05 was considered significant.

3. Results

3.1. Animal health and liver histology

The effects of PD, LD, and LED on body weights were not statistically significant (given in supplementary Figure 1). H&E and Oil Red O staining of the liver sections of rats fed

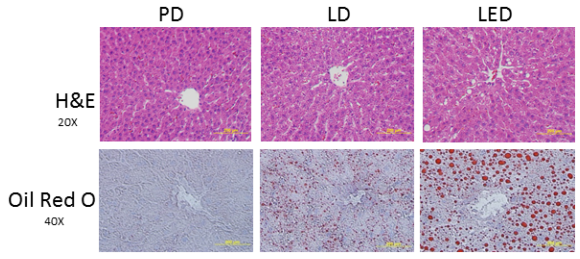

(a)

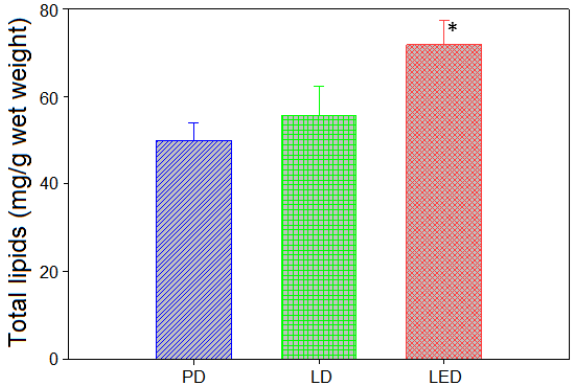

(b)

Figure 1: (a) The upper panel represents the H&E stained liver sections of PD, LD, and LED of SD rats fed 5% ethanol, respectively (original magnification X20) while the lower panel represents the Oil Red O stained liver sections of the same rats fed the three different diets (original magnification X40). Increased vacuolization and fat deposition were observed in the liver sections of LED. (b) Total dry lipid weights of livers of rats fed 5% ethanol daily for six weeks ($^*P$ value = .05 indicates significant). Data represent the mean $\pm$SD of $n = 6$ or 7.

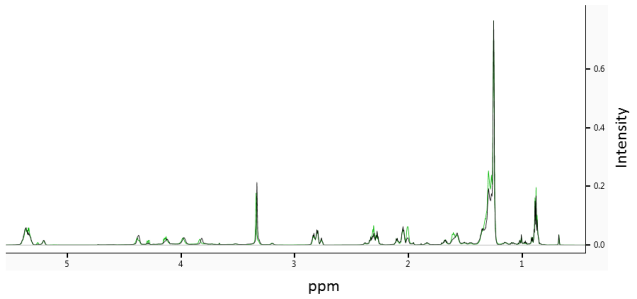

(a)

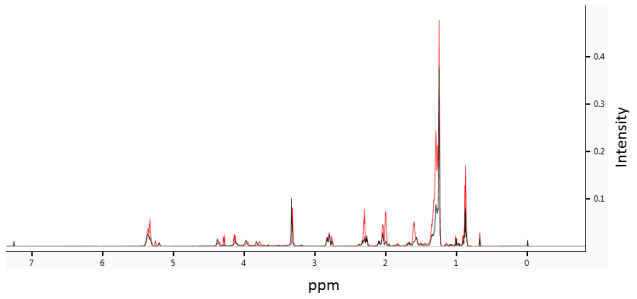

(b)

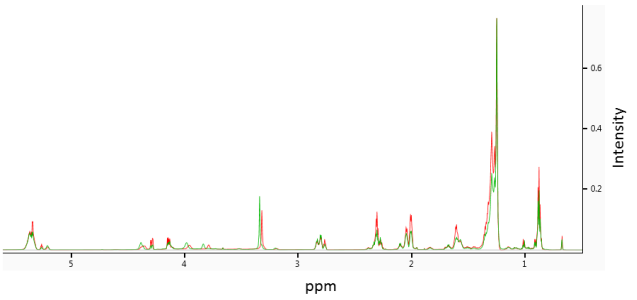

(c)

Figure 2: (a) Representative superimposed one-dimensional ^{1}H-NMR spectra (800 MHz) of lipid extracts from livers of PD and LD rats between -0.2 ppm and 5.5 ppm. TMS = 0.0 ppm PD (black) and LD (green). (b) Representative superimposed one-dimensional ^{1}H-NMR spectra (800 MHz) of lipid extracts from livers of PD and LED rats between -0.2 ppm and 7.2 ppm. TMS = 0.0 ppm PD (black) and LED (red). (c) Representative superimposed one-dimensional ^{1}H-NMR spectra (800 MHz) of lipid extracts from livers of LD and LED rats between -0.2 ppm and 5.5 ppm. TMS = 0.0 ppm LD (green) and LED (red).

the three diets are shown in Figure 1(a). Smaller fat accumulation was seen in the rats fed with PD as compared to the LD and LED. Mild fatty deposits were seen in the LD and LED fed rats while midzonal fatty infiltration was seen only in the rats fed LED. Lipid accumulation was further confirmed by the Oil Red O staining [16]. Lipid accumulation in the liver quantified by weighing extracted lipids to a constant dry weight and Oil Red O staining was used to demonstrate accumulation of lipids in hepatocytes. The grading scale of Tsukamoto et al. [18] as applied in our previous study could not differentiate between PD and LD groups because grade 1 indicates a wide range of 0%–25% hepatocytes with lipid droplets whereas differentiation in hepatocytes fat deposition was quantifiable in PD and LD groups by weighing extracted lipids dry weight from the liver.

The dry lipid weights of the livers shown in Figure 1(b) are consistent with the histological findings. No inflammation was observed in any group. Among liver injury markers (ALT, AST, ALP, and LDH) only ALT was significantly increased in LED group as compared to LD (data not shown). Increase in ALT level in plasma reflects only significant fatty changes as observed in LED group indicating initiation of liver injury as reported [30].

3.2. ^{1}H-NMR of liver lipids of rats fed different diets

Figure 2 shows the overlapping of representative NMR spectra of liver lipids from PD versus LD, PD versus LED,

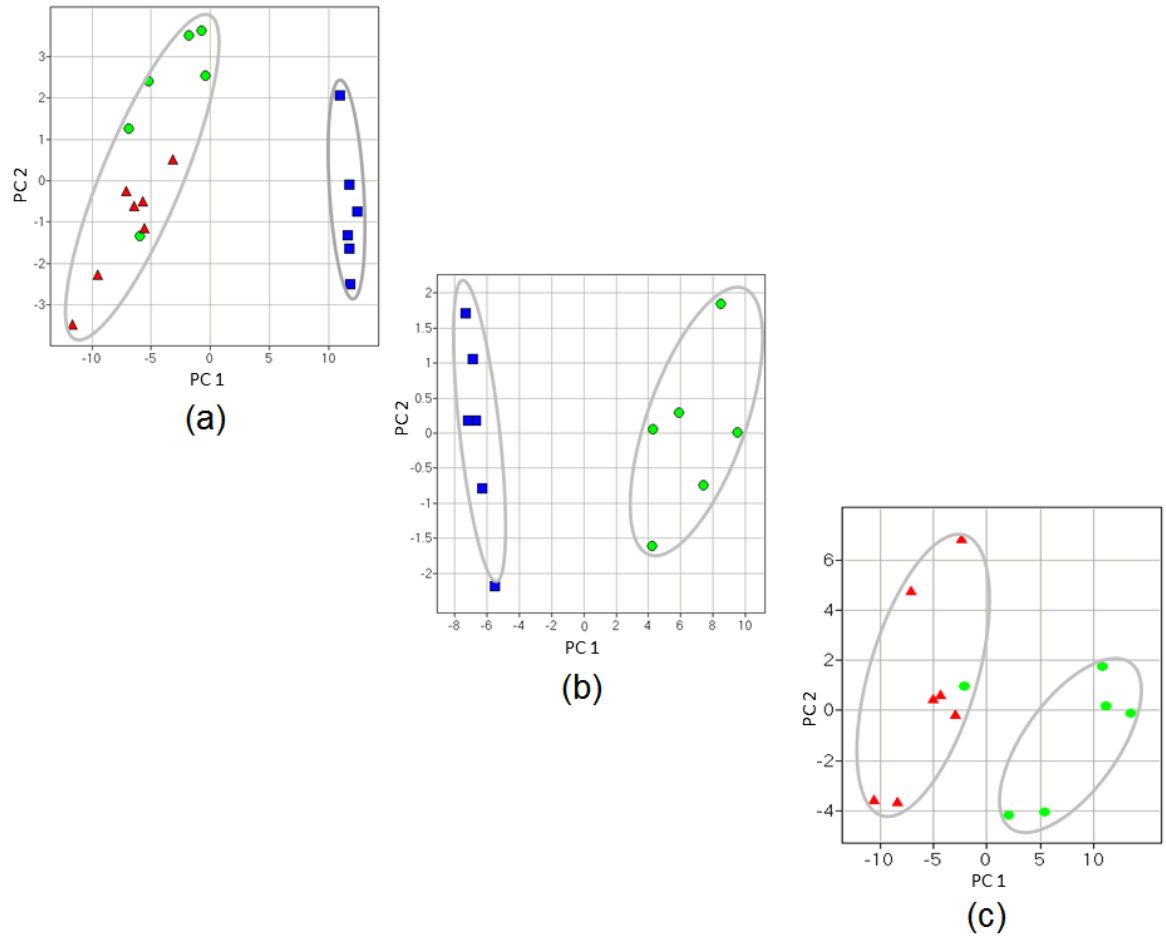

Figure 3: (a) PCA analysis of ^{1}H-NMR spectral data of lipids extracted from livers of PD (closed squares), LD (closed circles) and LED (closed triangles) fed SD rats for six weeks at $P = .01$. The two-dimensional plot of the data shows a clear separation of the PD fed rats from that of LD and LED fed rats. Herein, each point represents a value calculated from an individual spectrum. (b) PCA analysis of ^{1}H-NMR spectral data of lipids extracted from livers of PD (closed squares) and LD (closed circles) fed SD rats for six weeks at $P = .01$. The two-dimensional plot of the data shows a clear separation of the PD fed rats from that of LD fed rats. (c) PCA analysis of ^{1}H-NMR spectral data of lipids extracted from livers of LD (closed circles) and LED (closed triangles) fed SD rats for six weeks at $P = .01$. The two-dimensional plot of the data shows a clear separation of five LD fed rats from the LED fed rats. Herein, each point represents a value calculated from an individual spectrum. The significant changes associated with PD versus LD, PD versus LED, and LD versus LED are shown in Table 1.

and LD versus LED groups. The peaks of the representative spectra were assigned by comparison of chemical shifts to spectra reported in the literature as described in Section 2. Visual inspection of the spectra shows a clear difference between LD versus PD, LED versus PD, and LED versus LD groups. However, the differences are more pronounced in PD versus LED group than other comparisons. These changes correspond with the observed dry lipid weights (Figure 1(b)). To differentiate lipids patterns associated with different diets, multivariate data analysis was performed. The principal component analysis (PCA) profiles (Figure 3) of the lipids extracted from the livers of PD, LD, and LED groups show that in all comparisons, the separation of PD from either the LD or LED groups suggests that lipid profiles are altered either by LD or LED (Figures 3(a) and 3(b)). Figures 3(a) and 3(b) show the separation of LD and LED from PD, and Figure 3(c) shows the separation of LD from LED, which represents the effect of ethanol. In the comparison of LD versus LED, all rats were clustered together and are consistent with observed changes in signal intensities. Significant differences in the various comparisons could be observed at P values of 0.0001 for PD/LED, 0.001 in the PD/LD, while P values of 0.05 for the LD/LED comparison.

Table 1: Summary of altered significant lipid groups in the livers of high-fat diet versus PD, high-fat ethanol diet versus PD, and ethanol versus LD controls.

Lipid metabolite	Chemical shift (ppm)	PD versus LD (% change) ($P \leq .005$)	PD versus LED (% change) ($P \leq .0005$)	LD versus LED (% change) ($P \leq .05$)
Cholesterol (total)	0.68	+20	*NS*	**NS**
Cholesterol (C14 free)	0.97–0.99	−30, −39, −21	*−29*, *−42*, *−22*	**NS**
Free cholesterol	1.01	−12	*−21*	**−10**
Esterified cholesterol	1.02	+53	*+78*	**+16**
Cholesterol/fatty acyl chain $-CO-CH_2C\mathbf{H}_2-$	1.55–1.59	−21, −25, −26, −24	*−22*, *−24*, *−32*, *−33*, *−25*	**−12 (1.59)**
C3H of esterified cholesterol	4.61–4.63	NS	*NS*	**+48**, **+48**, **+53**
Cholesterol acetate (2.03)	2.00–2.03	+135, +162, +165, +76	*+163*, *+206*, *+212*, *+105*	**+12**, **+17**, **+18**, **+17**
Triglyceride $-C-1H_2$ in glycerol backbone	4.15–4.16	+52, +66	*+49*, *+68*	**NS**
Triglyceride $-C-3H_2$ in glycerol backbone	4.29–4.30, 4.31	+124, +100, +64	*+183*, *+138*, *+116*	**+26 (4.29)**, **+31 (4.31)**
Triglyceride −C−2H in glycerol backbone	5.26–5.27	+97, +121	*+119*, *+167*	**NS**
C−3H in glycerol phospholipid backbone	3.92, 3.93, 3.98, 4.04, **3.99–4.03**	−30, −37, −41, −25	*NS*	**−45**, **−63**, **−63**, **−51**, **−34**
C−1H in glycerol phospholipid backbone	4.05–4.13, *4.03–4.05*, *4.08*, *4.09*, *4.12*, *4.13*	−37, −44, −45, −43, −41, −46, −45, −41, −29	*−42*, *−35*, *−36*, *−41*, *−40*, *−34*, *−34*	**−10 (4.14)**
C−2H of glycerol phospholipid backbone	5.20–5.21, 5.24, 5.21–5.24, **5.22–5.23**, **5.24**	−52, −35, −24	*−39*, *−40*, *−43*, *−41*	**−26**, **−34**, **−21**
Terminal CH_3 gps in fatty acyl chain	0.89	+13	*+19*	**+5**
CH_2 in fatty acyl chain C4 and beyond (sat)	1.25, 1.26	−9 (1.25)	*−16 (1.26)*	**−12**, **−7**
CH_2 in fatty acyl chain C4 and beyond (sat)	1.27–1.31	+22, +31, +25, +32, +41	*+24*, *+39*, *+28*, *+43*, *+56*	**+6 (1.28)**, **+9 (1.30)**, **+10 (1.31)**
Fatty acyl chain $-COCH_2CH_2C\mathbf{H}_2-$	1.32–1.34	+51, +71, +47	*+70*, *+91*, *+67*	**+12**, **+12**, **+13**
CH_2 in acyl C3 (saturated chain) or $COCH_2C\mathbf{H}_2$	1.60–1.63	+27, +93, +116, +96	*+32*, *+120*, *+157*, *+128*	**+27**, **+93**, **+116**, **+96**
$-COO-CH_2-C\mathbf{H}_2-CH_2-CH=CH-$	1.67	−22	*−31*	**−22**
Fatty acyl chain $-CO-C\mathbf{H}_2CH_2-$	2.24, 2.25	−25, −28, −26 (2.28)	*−39*, *−36*, *−32 (2.28)*, *−37 (2.29)*	**−19 (2.24)**, **+11 (2.26)**, **+13 (2.27)**, **−22 (2.29)**
Fatty acyl chain $-CO-C\mathbf{H}_2CH_2-$	2.30–2.33, **2.31–2.33**	+19, +57, +73, +20	*+18*, *+80*, *+100*, *+32*	**+15**, **+16**, **+10**
Fatty acyl chain $-CO-C\mathbf{H}_2CH_2-$	2.36–2.39	−22, −30, −37, −38	*−28*, *−40*, *−41*, *−34*	**−10 (2.34)**, **−18 (2.35)**, **−14 (2.37)**
$-O-CH_3$ in methyl ester	3.78–3.81	NS	*NS*	**+22**, **+59**, **+123**, **+122**
Allylic $-CH=CH-C\mathbf{H}_2-$	2.0–2.03	+135, +162, +165, +76	*+163*, *+206*, *+212*, *+105*	**+12**, **+17**, **+18**, **+17**
Allylic $-CH=CH-C\mathbf{H}_2-$	2.04–2.10	−15, −14, −9, −13, −32, −32, −21	*−13*, *−11*, *−7*, *−11*, *−33*, *−30*, *−27*	**NS**
Diallylic $=CH-C\mathbf{H}_2-CH=$	2.76, 2.77, 2.80–2.86, *2.74–2.77*, *2.80*	−35, −21, −17, −14, −17, −21, −22, −34, −46	*−80*, *−65*, *−36*, *−16*, *−24*	**−10 (2.81)**
CH=CH in fatty acyl chain (unsaturated fatty acid)	5.34–5.35	+24, +32	*+29*, *+42*	**+7 (5.35)**
CH=CH in fatty acyl chain (unsaturated fatty acid)	5.36–5.39, *5.37–5.39*	−6, −13, −18, −19	*−13*, *−19*, *−20*	**NS**
$-N-CH_2-$ of phospatidylethanolamine	3.19, 3.20	−56, −38	*−41 (3.20)*, *−41 (3.25)*	**+54 (3.19)**, **−40 (3.21)**, **−47 (3.22)**
$P-O-CH_2-$ in choline/sphingomyelin	4.32–4.34, *4.29–4.31*, **4.36**, **4.37**	−39, −46, −56	*+183*, *+138*, *+116*	**+108**, **+40**
$-N^+(CH)_3$ of choline/sphingomyelin	3.30–3.33	NS	*NS*	**+49**, **+109**, **+103**, **+215**
$-CH_2-O-P$ in PE/LPE and/or POCH in PS	3.94–3.97	NS	*−41 (3.98)*	**+53**, **+98**, **+128**, **+85**
$-N^+(CH)_3$ of PC	3.35	NS	*NS*	**−86**
$-C\mathbf{H}_2-N^+(CH)_3$ of PC	3.84–3.86	NS	*NS*	**−69**, **−69**, **−70**
$P-O-C\mathbf{H}_2-$ in phosphatidylcholine	4.39–4.43	NS	*−62 (4.43)*	**−34**, **−56**, **−77**, **−70**, **−48**

NS = not significant.

The changes in PD versus LD, PD versus LED and LD versus LED are shown in normal font, italics and bold. If in a region ppm's were shifted, the bin values were marked with different fonts.

% change is calculated with the corresponding formula (or equation). For example % change A versus B = bin integration value of $(B-A)/A*100$. In each case, the A serves as a control for the comparison and we identified the changes of B with respect to A.

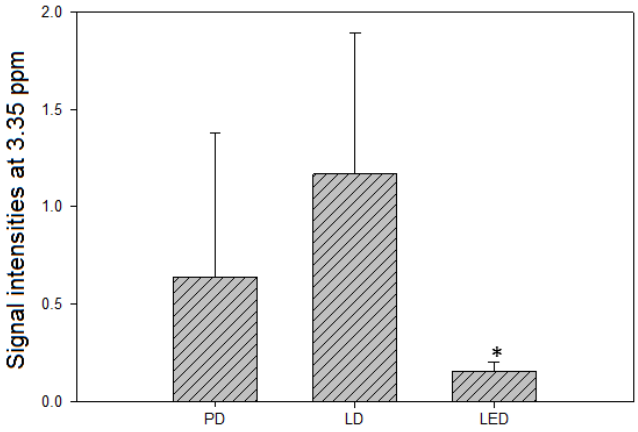

Figure 4: Intensity of the NMR signal at 3.35 ppm for rats fed the three different diets showing the differences among the three diets. ($^*P$-value $= .05$ indicates significant). Data represents the mean $\pm$SD of $n = 6$ or 7.

The changes in the NMR signal intensities and clustering patterns resulted in identification of different lipids as shown in Table 1. In all comparisons (PD vs. LD, PD vs. LED, and LD vs. LED), the NMR signals corresponding to esterified cholesterol (1.02 ppm) and cholesterol acetate (2.03 ppm) were higher in LED group. Protons corresponding to triglycerides were also significantly increased in LD and LED groups compared to PD group. Other increased signals were corresponding to terminal $-CH_3$, protons of saturated and unsaturated carbons, and allylic protons. Protons related to phospholipids are also shown in Table 1. The protons of the $-O-CH_3$ group increased only in LD versus LED comparison. The decreased signals resulted for free cholesterol, and protons of the phospholipid backbone in all the three comparisons, while phosphatidylcholine (PC)-related protons showed a decrease only in the LD versus LED comparison (Figure 4). Other signals of interest include changes observed in protons of $-CH_2-CO-$ corresponding to the fatty acids.

To compare the changes associated with fatty liver due to high fat diet or due to ethanol we considered the changes described in columns 1 (PD vs. LD) and 3 (LD vs. LED) of Table 1, and it showed changes in free cholesterol, esterified cholesterol, and cholesterol acetate, and the changes associated with lipid backbone of phospholipids and many other lipids are similar in both groups. Changes in triglyceride protons are more pronounced in LD group (high fat diet) than in the ethanol (LED) while changes associated with methyl ester protons, PC, and phosphatidylethanolamine (PE) are more dominant in the LED group.

4. Discussion

The alcohol-induced fatty liver development and progression studies have extensively used Lieber-DeCarli LD model in mice or rats [17,31,32,33]. In our earlier work, we used LD model and compared the changes in animals fed ethanol in high-fat liquid diet (LED) [12,13,14,15]. However, we did not compare with a PD as control to differentiate the changes in ethanol-fed animals originating from high-fat LD itself [13,14,16]. Formation of greater amounts of triglyceride represents a protecting role by blunting the flux of free fatty acids related to toxicity in the liver [34]. Fatty acids are known to cause injury via oxidative stress and inflammatory pathways [35].

In the present work, we evaluated how the fat diet and ethanol play a role in liver toxicity. Understanding the mechanism of fatty liver formation due to the diet is also important because of increased consumption of high-fat diet leading to NAFLD, obesity, and diabetes [36,37,38,39]. Hepatic steatosis is reported $\sim 70\%$ among type 2 diabetic patients with symptoms of the metabolic syndrome [40]. Dietary fat plays a critical role in the pathogenesis of NAFLD and ALD. Most of the NAFLD models utilize diets containing 20%–60% fat calories that are mainly derived from saturated fats. However, LD is composed of mainly unsaturated fats containing corn, olive, and safflower oils providing 35% of total calories. PD, used as a standard control diet in our experiment, is a versatile rodent diet designed for laboratory rat. Fat in the PD mostly comes from porcine animal fat, soya bean oil, saturated fatty acid, monounsaturated fatty acids by providing $\sim 12\%$ calories via fat. Dietary saturated fat has a protective effect whereas dietary unsaturated fat has deleterious effects on alcohol-induced liver pathology [41, 42,43]. However, the underlying mechanism(s) by which different types of dietary fat potentiate or attenuate ALD is not fully understood.

To differentiate the hepatic steatosis occurring due to high-fat diet or ethanol consumption is not currently available and diagnosis is largely confined to the patient's history of alcohol consumption. Therefore, it is important to device a method which can differentiate the genesis of hepatic steatosis using noninvasive methods. Metabolomics offers one such approach to identify a panel of biomarkers which could be promising [4,44,45,46] in the event where identifying a single biomarker molecule was not successful.

We employed proton NMR spectroscopy in conjunction with multivariate statistical analysis to identify the altered lipids associated with high fat LD and LED. A study of this nature is necessary as we need to understand and distinguish the lipidomic changes arising from a fatty diet or due to consumption of alcohol with high fat LD. Our study indicates that even though we did not observe a statistically significant difference in the body weight of the three groups of animals fed either PD, LD or LED, however various diets have differentially caused changes in the liver histology. The fat deposits observed by H&E staining and confirmed by Oil Red O staining were consistent with altered lipid

profiles. Interestingly, the lipid groups altered by LD or LED showed varied patterns. LD itself has a potential to induce varied patterns of ethanol-induced disease [31]. In our earlier work, 5% ethanol in LD was fed to rats and pattern recognition analysis was performed to differentiate the lipid profiles involved in progressive alcoholic fatty liver using Fischer rats after feeding ethanol for six weeks and one, two, and three months [13,14,16]. In this study, Sprague-Dawley rats were monitored for fatty changes after six weeks of ethanol exposure and compared with PD group to determine the changes associated with diet and ethanol. In most alcohol-related experiments, Lieber-DeCarli LD is used and the amount of calories from ethanol is substituted by maltose-dextrin as control. However, as shown in supplementary Table 1, the calories from fat content in LD and LED groups are both at 35% while in PD only 12%. The carbohydrate and protein-related calories are higher in PD while remained similar in LD and LED. The other major difference in LED and LD groups was alcohol (36% calories) in LED while it is substituted by maltose-dextrin in LD. In LED, 36% calories are derived from 5% alcohol is substituted in LD by adding maltose dextrin to provide equivalent calories.

So far there is no proper definition of high-fat diet [47]. Currently, different high calorie diets with fat percentages varying from 20% to 60% originating from different sources are used as high-fat diets [48]. In an earlier work on metabolic profiling of urine using NMR spectroscopy for diet-induced obesity in a mouse model, high-fat (HF) and high carbohydrate (HC) diets were used [7]. The HC diet caused a slow rate of weight gain and resulted in the activation of the tricarboxylic acid cycle [7]. However, the HF diet affected the nicotinamide metabolism. Ethanol containing LD is relatively more suitable for mimicking fatty liver injury while the catabolism of ethanol is about five times higher in rodents than those in humans. It has been shown previously that LD induces fatty liver in mice after four weeks of feeding and hence our results are consistent with earlier findings [47]. The intrahepatic free fatty acid metabolism in humans and animal models are highly complex. Fatty acid concentrations in the liver are controlled by many factors such as dietary intake, intrahepatic storage, β-oxidation, and export of newly synthesized fatty acids. So searching a biomarker profile in the livers of animals fed LD or LED resulting in fatty liver is rather complex.

Our finding that altered lipid signatures of PC decreases in LED group as compared to LD and PD groups is consistent with our earlier findings, where decreases in PC in LED as compared to LD group was observed in the liver and plasma [13]. Therefore, decreased PC levels in the liver as well as in the plasma can be a consistent observation in LED group, which offers an opportunity to be explored for identification of alcoholic fatty liver from NAFLD, a distinguishing feature between alcoholic versus nonalcoholic fatty liver. Further evidence to such observation can be supported by supplementing the finding with the analysis of circulating biomarkers of alcohol consumption [49]. Since PC is formed via different mechanisms together with its conversion to triglycerides, we speculate that decreased formation of PC is attributed to reduced methylation via PE primarily due to decreased levels of cofactor S-adenosyl methionine in alcoholics [50, 51,52]. PC and PE are major phospholipids found in mammalian cell membrane. The ratio of PC to PE is a regulator of cell membrane integrity and function. Increased PE exposure on cell surface causes a loss of membrane integrity and decreased PC/PE ratio plays a key role in progress of steatosis into steatohepatitis. This has clinical relevance since patients with nonalcoholic steatohepatitis have a decreased ratio of PC to PE compared to the control livers [53]. Similarly, lipid dysregulation influences the membrane integrity that leads to toxic metabolites released in hepatic parenchyma and provides a lipid signature in nonalcoholic steatohepatitis patients [54]. However, before exploring the effect of decreased PC as an indicator/marker of alcoholic fatty liver, these present findings in our study need to be further confirmed with a large number of animals and patient studies by targeted analysis of PC.

Acknowledgments This publication is financially supported by NIH Grant no. R01AA016364 (GASA) and AA025850 (BSK) and its contents are solely the responsibility of the authors and do not necessarily represent the views of the NIH or NIAAA. The authors would like to thank the following: Dr. Tianzhi Wang, manager, NMR Center of the Sealy Center for Structural Biology and Molecular Biophysics at UTMB, for the use of NMR instruments; Ms Mala Sinha, UTMB Bioinformatics Program for the availability of Spotfire program.

Conflict of interest The authors declare that they have no conflict of interest.

References

[1] A. Keegan, R. Martini, and R. Batey, *Ethanol-related liver injury in the rat: a model of steatosis, inflammation and pericentral fibrosis*, J Hepatol, 23 (1995), 591–600.

[2] J. Trebicka, I. Racz, S. V. Siegmund, E. Cara, M. Granzow, R. Schierwagen, et al., *Role of cannabinoid receptors in alcoholic hepatic injury: steatosis and fibrogenesis are increased in CB_2 receptor-deficient mice and decreased in CB_1 receptor knockouts*, Liver Int, 31 (2011), 860–870.

[3] H. Huang, M. Z. Akhtar, R. Ploeg, and B. M. Kessler, *Lipidomics techniques and its applications in medical research*, J Glycomics Lipidomics, 4 (2014), 2153–0637.

[4] J. K. Nicholson, J. Connelly, J. C. Lindon, and E. Holmes, *Metabonomics: a platform for studying drug toxicity and gene function*, Nat Rev Drug Discov, 1 (2002), 153–161.

[5] N. Zamboni, A. Saghatelian, and G. Patti, *Defining the metabolome: size, flux, and regulation*, Mol Cell, 58 (2015), 699–706.

[6] C. Paiva, A. Amaral, M. Rodriguez, N. Canyellas, X. Correig, J. L. Ballesca, et al., *Identification of endogenous metabolites in human sperm cells using proton nuclear magnetic resonance (^{1}H-NMR) spectroscopy and gas chromatography-mass spectrometry (GC-MS)*, Andrology, 3 (2015), 496–505.

[7] J.-Y. Jung, I.-Y. Kim, Y.-N. Kim, J.-S. Kim, J.-H. Shin, Z.-H. Jang, et al., *^{1}H-NMR-based metabolite profiling of diet-induced obesity in a mouse mode*, BMB Rep, 45 (2012), 419–424.

[8] S. H. Kim, S. O. Yang, H. S. Kim, Y. Kim, T. Park, and H. K. Choi, *^{1}H-nuclear magnetic resonance spectroscopy-based metabolic assessment in a rat model of obesity induced by a high-fat diet*, Anal Bioanal Chem, 395 (2009), 1117–1124.

[9] J. Pinto, L. M. Almeida, A. S. Martins, D. Duarte, A. S. Barros, E. Galhano, et al., *Prediction of gestational diabetes through NMR metabolomics of maternal blood*, J Proteome Res, 14 (2015), 2696–2706.

[10] A. C. Gavin, K. Maeda, and S. Kuhner, *Recent advances in charting protein-protein interaction: mass spectrometry-based approaches*, Curr Opin Biotechnol, 22 (2011), 42–49.

[11] Z. Huang, W. Shao, J. Gu, X. Hu, Y. Shi, W. Xu, et al., *Effects of culture media on metabolic profiling of the human gastric cancer cell line SGC7901*, Mol Biosyst, 11 (2015), 1832–1840.

[12] T. I. Lopes, B. Geloneze, J. C. Pareja, A. R. Calixto, M. M. Ferreira, and A. J. Marsaioli, *Blood metabolome changes before and after bariatric surgery: A ^{1}H-NMR-based clinical investigation*, OMICS, 19 (2015), 318–327.

[13] H. Fernando, S. Kondraganti, K. K. Bhopale, D. E. Volk, M. Neerathilingam, B. S. Kaphalia, et al., *^{1}H and ^{31}p NMR lipidome of ethanol-induced fatty liver*, Alcohol Clin Exp Res, 34 (2010), 1937–1947.

[14] H. Fernando, K. K. Bhopale, S. Kondraganti, B. S. Kaphalia, and G. A. Shakeel Ansari, *Lipidomic changes in rat liver after long-term exposure to ethanol*, Toxicol Appl Pharmacol, 255 (2011), 127–137.

[15] H. Fernando, K. K. Bhopale, P. J. Boor, G. A. Shakeel Ansari, and B. S. Kaphalia, *Hepatic lipid profiling of deer mice fed ethanol using ^{1}H and ^{31}P NMR spectroscopy: a dose-dependent subchronic study*, Toxicol Appl Pharmacol, 264 (2012), 361–369.

[16] K. K. Bhopale, S. Kondraganti, H. Fernando, P. J. Boor, B. S. Kaphalia, and G. A. Shakeel Ansari, *Alcoholic steatosis in different strains of rat: A comparative study*, J Drug Alcohol Res, 4 (2015), 1–9.

[17] C. Lieber and L. DeCarli, *Liquid diet technique of ethanol administration: 1989 update*, Alcohol Alcohol, 24 (1989), 197–211.

[18] H. Tsukamoto, S. W. French, N. Benson, G. Delgado, G. A. Rao, E. C. Larkin, et al., *Severe and progressive steatosis and focal necrosis in rat liver induced by continuous intragastric infusion of ethanol and low fat diet*, Hepatology, 5 (1985), 224–232.

[19] D. Chapman and A. Morrison, *Physical studies of phospholipids. IV. High resolution nuclear magnetic resonance spectra of phospholipids and related substances*, J Biol Chem, 241 (1966), 5044–5052.

[20] R. A. Awl, E. N. Frankel, and D. Weisleder, *Synthesis and characterization of triacylglycerols containing linoleate and linolenate*, Lipids, 24 (1989), 866–872.

[21] D. Y. Sze and O. Jardetzky, *Characterization of lipid composition in stimulated human lymphocytes by ^{1}H-NMR*, Biochim Biophys Acta, 1054 (1990), 198–206.

[22] E. Hatzakis, A. Koidis, D. Boskou, and P. Dais, *Determination of phospholipids in olive oil by ^{31}P-NMR spectroscopy*, J Agric Food Chem, 56 (2008), 6232–6240.

[23] M. S. Jie and K. L. Cheng, *Nuclear magnetic resonance spectroscopic analysis of homoallylic and bis homoallylic substituted methyl fatty ester derivatives*, Lipids, 30 (1995), 115–120.

[24] G. Knothe, *Nuclear magnetic resonance spectroscopy*, in The Lipid Handbook, F. D. Gunstone, J. L. Harwood, and A. J. Dijkstra, eds., CRC Press, Boca Raton, FL, 2007, 455–459.

[25] M. Oostendorp, U. F. Engelke, M. A. Willemsen, and R. A. Wevers, *Diagnosing inborn errors of lipid metabolism with proton nuclear magnetic resonance spectroscopy*, Clin Chem, 52 (2006), 1395–1405.

[26] P. Pollesello, F. Masutti, L. S. Croce, R. Toffanin, O. Eriksson, S. Paoletti, et al., *^{1}H-NMR spectroscopic studies of lipid extracts from human fatty liver*, Biochem Biophys Res Commun, 192 (1993), 1217–1222.

[27] V. Tugnoli, G. Bottura, G. Fini, A. Reggiani, A. Tinti, A. Trinchero, et al., *^{1}H-NMR and ^{13}C-NMR lipid profiles of human renal tissues*, Biopolymers, 72 (2003), 86–95.

[28] L. Wei, P. Liao, H. Wu, X. Li, F. Pei, W. Li, et al., *Toxicological effects of cinnabar in rats by NMR-based metabolic profiling of urine and serum*, Toxicol Appl Pharmacol, 227 (2008), 417–429.

[29] R. Teschke, M. Neuefeind, M. Nishimura, and G. Strohmeyer, *Hepatic gamma-glutamyltransferase activity in alcoholic fatty liver: comparison with other liver enzymes in man and rats*, Gut, 24 (1983), 625–630.

[30] W. K. Wilson, R. M. Sumpter, J. J. Warren, P. S. Rogers, B. Ruan, and G. J. Schroepfer, *Analysis of unsaturated C27 sterols by nuclear magnetic resonance spectroscopy*, J Lipid Res, 37 (1996), 1529–1555.

[31] C. Lieber, L. Decarli, and M. F. Sorrell, *Experimental methods of ethanol administration*, Hepatology, 10 (1989), 501–510.

[32] B. U. Bradford, T. M. O'Connell, J. Han, O. Kosyk, S. Shymonyak, P. K. Ross, et al., *Metabolomic profiling of a modified alcohol liquid diet model for liver injury in the mouse uncovers new markers of disease*, Toxicol Appl Pharmacol, 232 (2008), 236–243.

[33] K. K. Bhopale, H. Wu, P. J. Boor, V. L. Popov, G. A. Ansari, and B. S. Kaphalia, *Metabolic basis of ethanol-induced hepatic and pancreatic injury in hepatic alcohol dehydrogenase deficient deer mice*, Alcohol, 39 (2006), 179–188.

[34] K. Yamaguchi, L. Yang, S. McCall, J. Huang, X. X. Yu, S. K. Pandey, et al., *Inhibiting triglyceride synthesis improves hepatic steatosis but exacerbates liver damage and fibrosis in obese mice with nonalcoholic steatohepatitis*, Hepatology, 45 (2007), 1366–1374.

[35] C. J. McClain, S. Barve, and I. Deaciuc, *Good fat/bad fat*, Hepatology, 45 (2007), 1343–1346.

[36] Z. M. Younossi, D. Blissett, R. Blissett, L. Henry, M. Stepanova, Y. Younossi, et al., *The economic and clinical burden of nonalcoholic fatty liver disease in the United States and Europe*, Hepatology, 64 (2016), 1577–1586.

[37] G. Targher, F. Valbusa, S. Bonapace, L. Bertolini, L. Zenari, S. Rodella, et al., *Non-alcoholic fatty liver disease is associated with an increased incidence of atrial fibrillation in patients with type 2 diabetes*, PLoS One, 8 (2013), e57183.

[38] M. Charlton, *Nonalcoholic fatty liver disease: a review of current understanding and future impact*, Clin Gastroenterol Hepatol, 2 (2004), 1048–1058.

[39] R. Vuppalanchi and N. Chalasani, *Nonalcoholic fatty liver disease and nonalcoholic steatohepatitis: Selected practical issues in their evaluation and management*, Hepatology, 49 (2009), 306–317.

[40] J. K. Dowman, J. W. Tomlinson, and P. N. Newsome, *Pathogenesis of non-alcoholic fatty liver disease*, QJM, 103 (2010), 71–83.

[41] I. A. Kirpich, M. E. Miller, M. C. Cave, S. Joshi-Barve, and C. J. McClain, *Alcoholic liver disease: update on the role of dietary fat*, Biomolecules, 6 (2016), 1.

[42] A. A. Nanji, *Role of different dietary fatty acids in the pathogenesis of experimental alcoholic liver disease*, Alcohol, 34 (2004), 21–25.

[43] E. Mezey, *Dietary fat and alcoholic liver disease*, Hepatology, 28 (1998), 901–905.

[44] F. Courant, J. P. Antignac, F. Monteau, and B. Le Bizec, *Metabolomics as a potential new approach for investigating human reproductive disorders*, J Proteome Res, 12 (2013), 2914–2920.

[45] O. Beckonert, H. C. Keun, T. M. Ebbels, J. Bundy, E. Holmes, J. C. Lindon, et al., *Metabolic profiling, metabolomic and*

metabonomic procedures for NMR spectroscopy of urine, plasma, serum and tissue extracts, Nat Protoc, 2 (2007), 2692–2703.

[46] J. B. German, L. A. Gillies, J. T. Smilowitz, A. M. Zivkovic, and S. M. Watkins, *Lipidomics and lipid profiling in metabolomics*, Curr Opin Lipidol, 18 (2007), 66–71.

[47] P. Ramadori, R. Weiskirchen, J. Trebicka, and K. Streetz, *Mouse models of metabolic liver injury*, Lab Anim, 49 (2015), 47–58.

[48] R. Buettner, J. Scholmerich, and L. C. Bollheimer, *High-fat diets: modeling the metabolic disorders of human obesity in rodents*, Obesity (Silver Spring), 15 (2007), 798–808.

[49] R. Z. Litten, A. M. Bradley, and H. B. Moss, *Alcohol biomarkers in applied settings: recent advances and future research opportunities*, Alcohol Clin Exp Res, 34 (2010), 955–967.

[50] V. Purohit, M. F. Abdelmalek, S. Barve, N. J. Benevenga, C. H. Halsted, N. Kaplowitz, et al., *Role of S-adenosylmethionine, folate, and betaine in the treatment of alcoholic liver disease: summary of a symposium*, Am J Clin Nutr, 86 (2007), 14–24.

[51] R. L. Jacobs, J. N. van der Veen, and D. E. Vance, *Finding the balance: the role of S-adenosylmethionine and phosphatidylcholine metabolism in development of nonalcoholic fatty liver disease*, Hepatology, 58 (2013), 1207–1209.

[52] M. Martínez-Uña, M. Varela-Rey, A. Cano, L. Fernández-Ares, N. Beraza, I. Aurrekoetxea, et al., *Excess S-adenosylmethionine reroutes phosphatidylethanolamine towards phosphatidylcholine and triglyceride synthesis*, Hepatology, 58 (2013), 1296–1305.

[53] Z. Li, L. B. Agellon, T. M. Allen, M. Umeda, L. Jewell, A. Mason, et al., *The ratio of phosphatidylcholine to phosphatidylethanolamine influences membrane integrity and steatohepatitis*, Cell Metab, 3 (2006), 321–331.

[54] F. Chiappini, A. Coilly, H. Kadar, P. Gual, A. Tran, C. Desterke, et al., *Metabolism dysregulation induces a specific lipid signature of nonalcoholic steatohepatitis in patients*, Sci Rep, 7 (2017), 46658.